

Moisture Condensation on Epitaxial Graphene upon Cooling

Muhammad Farooq Saleem ^{1,2}, Niaz Ali Khan ³, Muhammad Javid ⁴, Ghulam Abbas Ashraf ⁵, Yasir A. Haleem ⁶, Muhammad Faisal Iqbal ⁷, Muhammad Bilal ⁸, Peijie Wang ^{9,*} and Ma Lei ^{1,*}

¹ Tianjin International Center for Nanoparticles and Nanosystems, Tianjin University, Tianjin 300072, China

² GBA Branch of Aerospace Information Research Institute, Chinese Academy of Sciences, Guangzhou 510700, China

³ Hubei Key Laboratory of Advanced Textile Materials & Application, Wuhan Textile University, Yangguang Road 1, Wuhan 430200, China

⁴ Institute of Advanced Magnetic Materials, College of Materials and Environmental Engineering, Hangzhou Dianzi University, Hangzhou 310012, China

⁵ Key Laboratory of Integrated Regulation and Resources Development on Shallow Lake, Ministry of Education, College of Environment, Hohai University, Nanjing 210098, China

⁶ Department of Physics, Khwaja Fareed University of Engineering and Information Technology, Rahim Yar Khan 64200, Pakistan

⁷ Department of Physics, Riphah International University, Faisalabad 38000, Pakistan

⁸ College of Materials Science and Technology, Nanjing University of Aeronautics and Astronautics, Nanjing 210016, China

⁹ The Beijing Key Laboratory for Nano-Photonics and Nano-Structure, Department of Physics, Capital Normal University, Beijing 100048, China

* Correspondence: pjwan@cnu.edu.cn (P.W.); maleixinjiang@tju.edu.cn (M.L.)

Abstract: Condensation of moisture on the epitaxial graphene on 6H-SiC was observed below room temperature despite continuous nitrogen flow on the graphene surface. Raman peaks associated with ice were observed. A combination of peaks in the frequency range of 500–750 cm⁻¹, along with a broad peak centered at ~1327 cm⁻¹, were also observed and were assigned to airborne contaminants. The latter is more important since its position is in the frequency range where the defect-associated D band of graphene appears. This band can be easily misunderstood to be the D band of graphene, particularly when the Raman spectrum is taken below room temperature. This peak was even observed after the sample was brought back to room temperature due to water stains. This work highlights the importance of careful Raman investigation of graphene below room temperature and its proper insulation against moisture.

Keywords: epitaxial graphene; Raman scattering; condensation; adsorption

Citation: Saleem, M.F.; Khan, N.A.; Javid, M.; Ashraf, G.A.; Haleem, Y.A.; Iqbal, M.F.; Bilal, M.; Wang, P.; Lei, M. Moisture Condensation on Epitaxial Graphene upon Cooling. *Technologies* **2023**, *11*, 30. <https://doi.org/10.3390/technologies11010030>

Academic Editors: Sergey N. Grigoriev, Marina A. Volosova and Anna A. Okunkova

Received: 25 November 2022

Revised: 8 February 2023

Accepted: 11 February 2023

Published: 13 February 2023



Copyright: © 2023 by the authors. Licensee MDPI, Basel, Switzerland. This article is an open access article distributed under the terms and conditions of the Creative Commons Attribution (CC BY) license (<https://creativecommons.org/licenses/by/4.0/>).

1. Introduction

The 2D materials have drawn considerable interest in the last few decades for their unique properties and important device applications [1]. Particularly, graphene has been studied widely compared with any other 2D material since its discovery [2]. Its exceptional carrier mobility and favorable electronic properties have attracted much interest of device fabrication technology [3,4]. Graphene can be produced by physical and chemical methods [5]. Graphene of a precise number of layers can be achieved by optimizing the growth recipes on metal, semiconducting and insulating substrates by physical growth methods. CVD and epitaxial growth methods on solid surfaces have proved to be the most promising methods to obtain large area high-quality graphene. Graphene growth on technologically important SiC substrate has been achieved on both the Si and C-faces. The properties of graphene on two faces are affected by the type of plane on which it is grown. Graphene on the Si-face is particularly different due to an unavoidable underlying buffer layer of carbon that grows between the graphene and silicon face during the growth pro-

cess. Charge transfer and substrate interaction of graphene on the Si-face affect its properties more compared with the C-face. However, poor control over the number of graphene layers is the key issue on the C-face that usually yields thick graphene layers. Although the focus of this research is on graphene growth on the Si-face for its controllability on the number of layers, graphene on the C-face exhibits higher carrier mobility that makes it superior [6]. The carrier mobility of graphene is highly influenced by the number of layers; therefore, growth control is technologically very important [7,8].

The change in ambient temperature and interaction of environmental species can strongly affect the properties of atomically thin and sensitive graphene layers, which make it the material of choice for sensing applications. Graphene's wetting properties have been studied extensively and a clear change in its wetting properties has been observed simply by surface functionalizing. Many studies have given controversial and inconsistent results about graphene properties and the performance of graphene based devices so far [9]. The surface charge, defects and adsorbates are considered to be the sources of inconsistent graphene properties [9,10]. The intentional adsorption of known molecular species on graphene surfaces results in controlled doping and modification of its various electrical and optical properties. However, the unintentional adsorption of unknown ambient species can lead to degradation, inconsistent device behaviors, and poor reliability of graphene-based devices. The single-atom thick graphene surface exposed to air can have bulk aerosol and moisture deposits. Such materials trapped in moisture are more likely to adsorb on open surfaces, particularly below room temperature. It is indeed very important to keep the surface clear to be able to benefit from the intrinsic properties of highly sensitive graphene layers. In this study, we observed a change in the Raman spectrum of epitaxial graphene upon cooling due to moisture condensation on its surface that is significant and can result in the misleading evaluation of its quality if dealt with carelessly. For quality assurance and stable graphene-based device behaviors, proper surface insulation is necessary below room temperature. Raman spectroscopy is one of the most sensitive techniques that has successfully detected the contamination deposition of the graphene surface. Further investigation with similar characterization techniques can allow the detection of contaminants and their effects on the properties of graphene-based devices.

2. Experimental

2.1. Materials

Vanadium-doped semi-insulating 6H-SiC substrate was purchased from Wolfspeed (4600 Silicon Drive Durham, North Carolina 27703, USA). The thickness of 6H-SiC substrate was 369 μm . The substrates were polished on both Si and C faces.

2.2. Epitaxial Graphene Growth

The 6H-SiC substrates were ultrasonically cleaned in acetone and ethanol prior to graphene growth. Graphene was grown in a home-made RF-furnace at 1550 $^{\circ}\text{C}$ on the atomically flat 6H-SiC substrate for 25 min in a high vacuum ($<10^{-10}$ Torr). At sufficiently high temperature, Si evaporates from the substrate leaving C atoms behind that form graphene. The main components of the furnace include a large copper coil, sample stage, quartz tube, a protective shield and an AC power supply. An alternating current is produced using the power supply in the middle RF range. It heats the sample placed in the tube. A turbo pump is used to evacuate the tube.

2.3. Measurements

Optical images of the graphene surface grown on the carbon face of the 6H-SiC substrate were taken using an optical microscope attached with RH13325 (R-2000) Raman spectrometer in the complete temperature cycle between room temperature and -180°C using a 50 \times objective lens. The 532 nm excitation laser with 2 μm spot size of the same

Raman spectrometer was used to obtain the in situ temperature-dependent Raman spectra of the graphene in the same temperature range. A 50× objective lens was used. The sample was placed in a hot/cold cell and the liquid nitrogen was passed on it while taking temperature-dependent Raman spectra and optical images of the graphene surface at atmospheric pressure. The Raman spectra and optical images were taken after every 30 °C change in temperature continuously in the complete temperature cycle. The temperature was allowed to stabilize before each spectrum was obtained. Low room temperature and the humid lab environment allowed increased moisture condensation on the sample surface as shown in Figure 1. High vacuum annealing of the graphene sample was performed at 500 °C before Raman spectra and optical images were taken to clean any contaminants from the graphene sample surface.

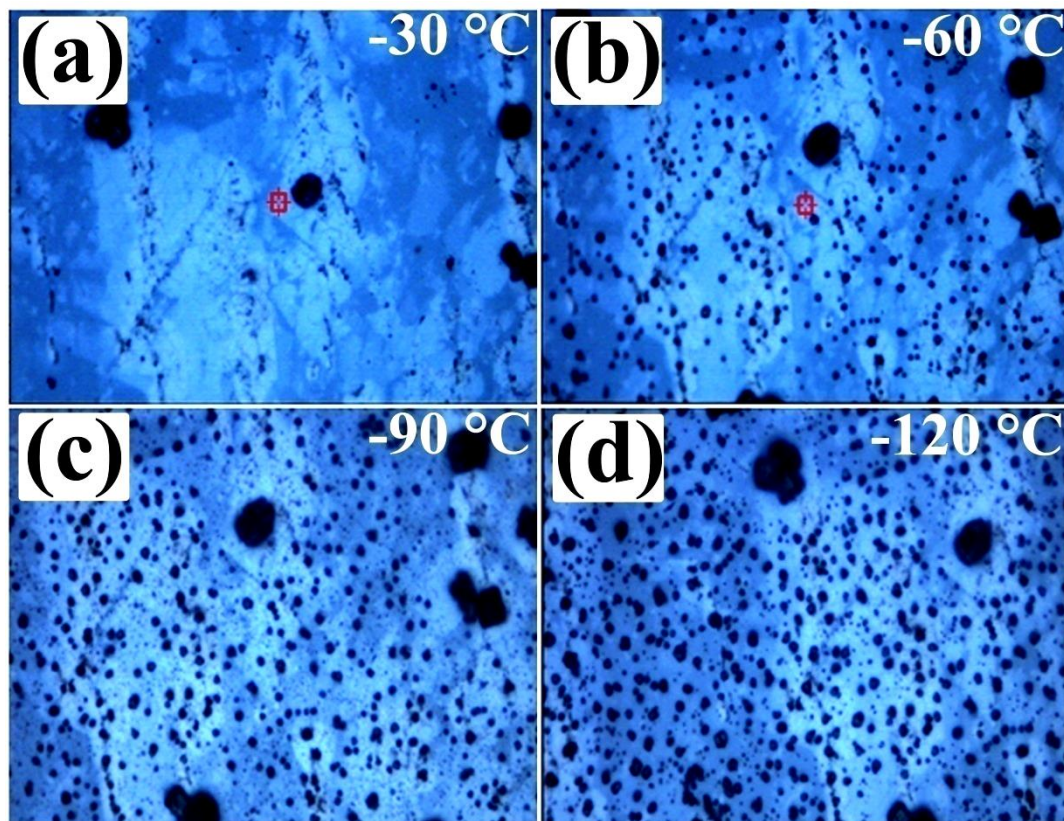


Figure 1. Optical microscopy images of the epitaxial graphene at (a) $-30\text{ }^{\circ}\text{C}$, (b) $-60\text{ }^{\circ}\text{C}$, (c) $-90\text{ }^{\circ}\text{C}$, and (d) $-120\text{ }^{\circ}\text{C}$ temperatures.

3. Results and Discussion

The epitaxial graphene on 6H-SiC was annealed in a vacuum for 5 h to get rid of any moisture or contaminants before the temperature-dependent Raman spectra were obtained. However, graphene has been reported to be more chemically active for adsorption after vacuum annealing [11]. It is assumed that the adsorbates can be removed by annealing leaving active sites for more adsorbates to come which makes graphene more lipophilic. Graphene on the C-face of SiC contains wrinkles, ridges and ripples that can further facilitate adsorption [12].

Temperature-dependent Raman spectra were obtained in a complete cycle between room temperature and $-180\text{ }^{\circ}\text{C}$. The surface of the sample was continuously observed through the optical microscope attached with Raman spectroscopy. The moisture starts to condense on the surface of the sample upon cooling despite the continuous flow of nitrogen. When the temperature reaches near $-30\text{ }^{\circ}\text{C}$, the water droplets become noticeable on

the surface as shown in optical microscopy images in Figure 1. Only big and distant droplets appear at first. The smaller droplets start to appear on the surface between the big droplets with further cooling.

An apparently clear area between the droplets was chosen to take the temperature-dependent Raman spectra but the continuous moisture condensation attenuated the Raman signal of the sample. The Raman signal was lost continuously, and the focus adjustments were made after every few degrees centigrade change in temperature. A strong background in Raman spectra was observed upon cooling that was subtracted from all the spectra for clarity. Moisture condensation and contaminants can lead to fluorescence background [13]. The contaminations resulted in some peaks other than normal Raman peaks of graphene and SiC substrate. The peaks at 227, 293, 414, 550–750, 1327, and 3200 cm^{-1} are observed upon cooling below 0 °C and remain observable during the complete temperature cycle as shown in Figure 2a,b. The peaks are assigned to the moisture and contaminants it carries [14–17]. The broad feature in the range 550–750 cm^{-1} is a combination of peaks that is due to the complex form of contaminants in the moisture. The contaminants can be airborne aerosols such as dust, soot, smoke, pollen, etc., or a combination of them. The droplets were not observable through the microscope once the sample was brought back to room temperature. Figure 2c shows the comparison of the Raman spectra for the sample before and after the complete cooling cycle. The peaks related to moisture and contaminants remain evident even when the sample is heated back to room temperature. This confirms that complete desorption of moisture and contaminants does not occur upon heating the sample back to room temperature. The hydrated contaminants can only be cleaned by high vacuum annealing of the sample. The graphene stored at ambient pressure should be annealed in a vacuum once it faces temperatures below room temperature to restore its actual properties.

The peak near 1327 cm^{-1} is significant due to its position near the D band of graphene. Low-temperature Raman spectroscopy of graphene has been reported many times [18–20]. Intentional graphene surface functionalization and molecule adsorption has also been studied extensively [21–23]. The activation of D band only by cooling or contaminating/functionalizing the surface of graphene has never been reported. Thus, the possibility of this peak being a D band can be ruled out. The peak is assigned to the contaminants that moisture carries.

In many parts of the world, −30 °C is room temperature at some point. A low temperature is often maintained in laboratories to avoid excessive heating of equipment. Graphene exposed to such environments can easily attract pollutants present in the air. A peak near 1327 cm^{-1} can be easily misinterpreted as a D band of graphene in the graphene sample exposed to open air below room temperature. The D band is used as the most reliable measure of graphene quality [24]. Graphene surface should be carefully cleaned by high vacuum annealing before Raman analysis once the surface has faced a temperature below 0 °C in open air.

To further confirm the origin of the observed peaks, the Raman laser was focused on a big droplet on the graphene surface, and temperature-dependent Raman spectra were obtained as shown in Figure 3a. Intense and clear ice signals were observed in the range of 2800–3800 cm^{-1} with peaks at 227 and 1327 cm^{-1} [25]. The Raman peaks of graphene and SiC were also observed. The ice-related broad feature in the range of 2800–3800 cm^{-1} was fitted and gave the well-known four peaks associated with ice at 3205, 3113, 3221 and 3364 cm^{-1} as shown in Figure 3b. Interestingly, the previously observed features in the range of 550–750 cm^{-1} on a surface between the droplets were not observed this time. Only a small peak near 550 cm^{-1} was observed. The water droplets and contaminants may have their preferential adsorption sites. The type of contaminants that prefer to adsorb between the water droplets and give rise to Raman features in the range of 550–750 cm^{-1} do not adsorb on water droplet formation sites. Careful graphene surface characterization and proper insulation are, hence, important in low-temperature environments.

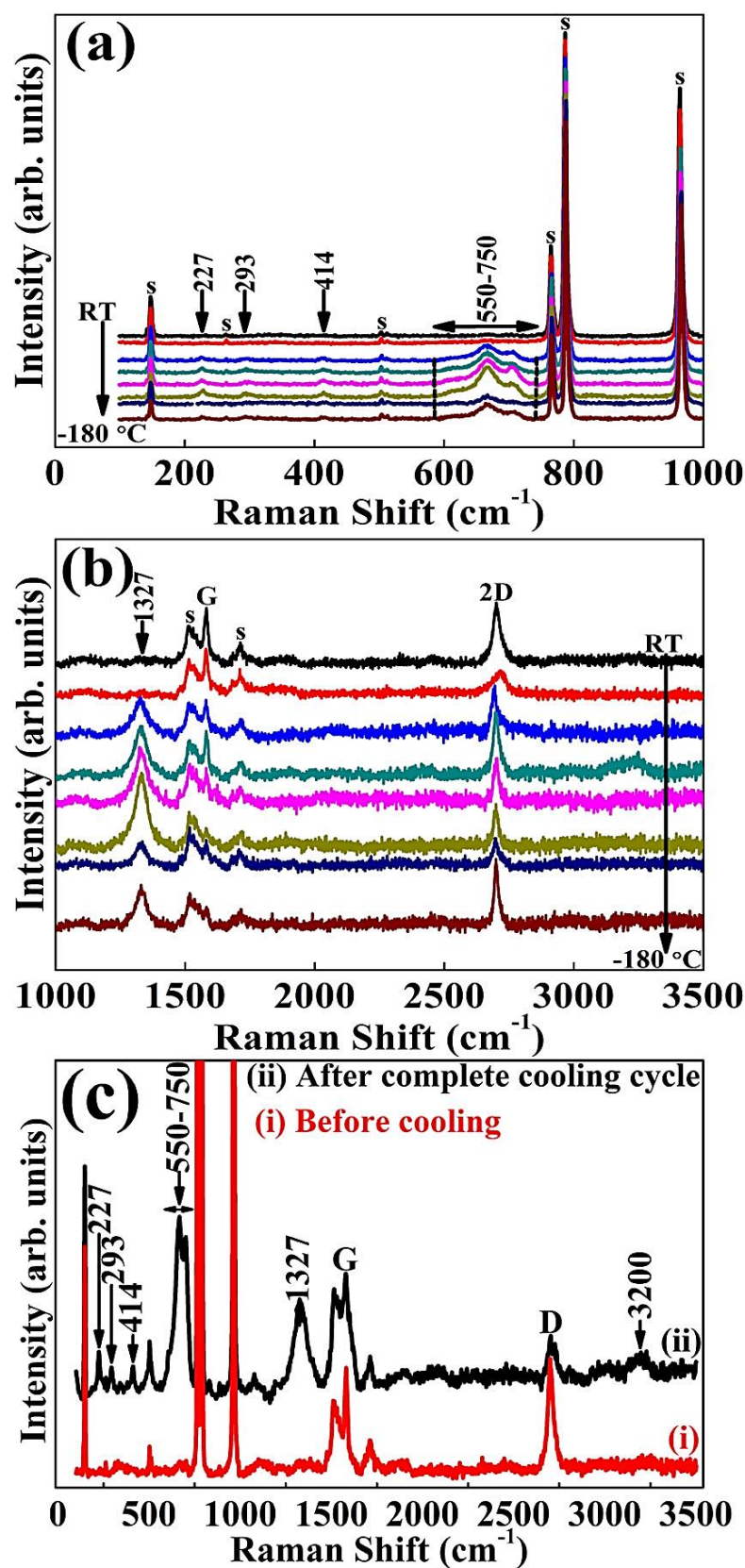


Figure 2. (a) Temperature-dependent Raman spectra recorded from room temperature to -180°C in Raman frequency range of $1000\text{--}3500\text{ cm}^{-1}$. (b) Temperature-dependent Raman spectra were recorded from room temperature to -180°C in the Raman frequency range of $100\text{--}1000\text{ cm}^{-1}$. (c) Raman spectra of epitaxial graphene were taken at room temperature before and after the cooling cycle.

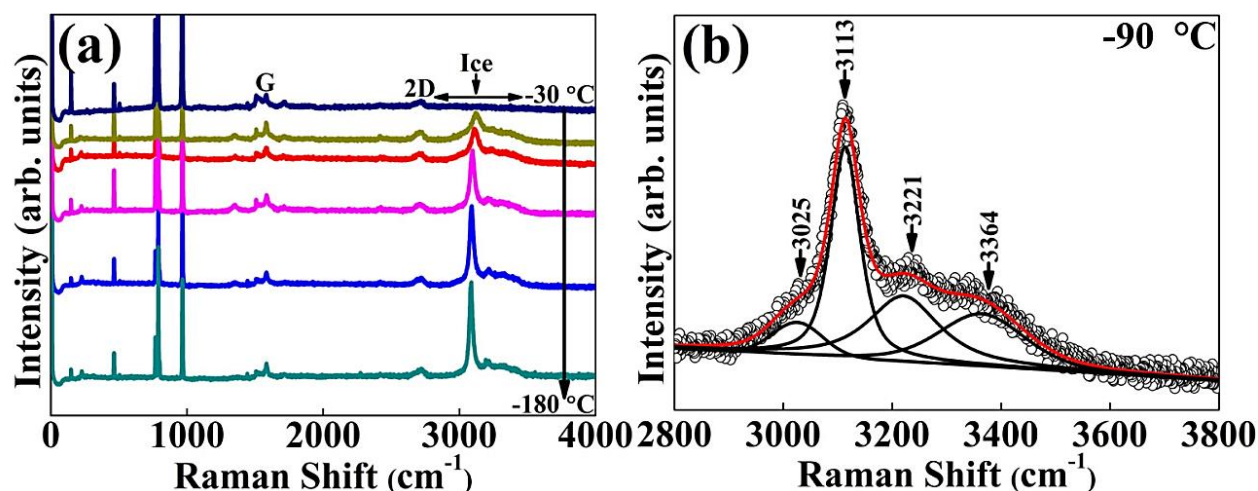


Figure 3. (a) Temperature-dependent Raman spectra obtained by focusing the laser to a frozen water droplet (b) fitting of the water-related peak obtained at $-90\text{ }^{\circ}\text{C}$.

4. Conclusions

Condensation of moisture on the epitaxial graphene on 6H-SiC was investigated by Raman spectroscopy below room temperature. The Raman spectra showed the Raman peaks associated with ice and contaminants below $0\text{ }^{\circ}\text{C}$. A peak near 1327 cm^{-1} associated with contaminants is particularly important for its position since it is in the frequency range where the D band of graphene occurs. The D band is usually used as the most reliable measure of graphene quality. Careful Raman investigation of graphene and its insulation against moisture is, therefore, important below $0\text{ }^{\circ}\text{C}$. Proper investigation of the abundant species in the air can provide a clear understanding of the contaminants and their possible effects on graphene's intrinsic properties that should be explored further by using sensitive characterization techniques similar to Raman spectroscopy.

Author Contributions: Conceptualization, M.F.S. and M.L.; methodology, M.F.S.; software, G.A.A., M.J., Haleem Y.A.H.; validation, M.L., M.F.I. and M.B.; formal analysis, P.W., M.F.S., and M.L.; investigation, Y.A.H., M.F.S., M.J., and G.A.A.; resources, M.L., N.A.K., P.W.; data curation, M.F.S., Y.A.H. and M.B.; writing—original draft preparation, M.F.S., M.L., M.F.I., and M.J.; writing—review and editing, M.B.; M.F.I. visualization, M.B., M.F.I., and M.J.; supervision, M.L., P.W. and M.F.S.; project administration, M.L. and P.W.; funding acquisition, M.L. and P.W. All authors have read and agreed to the published version of the manuscript.

Funding: This research received no external funding.

Institutional Review Board Statement: Not applicable.

Informed Consent Statement: Not applicable.

Data Availability Statement: All the data taken in this work has been published in this paper.

Conflicts of Interest: The authors declare that they have no conflict of interest.

References

1. Mondal, B.; Gogoi, P.K. Nanoscale Heterostructured Materials Based on Metal Oxides for a Chemiresistive Gas Sensor. *ACS Appl. Electron. Mater.* **2022**, *4*, 59–86. <https://doi.org/10.1021/acsaem.1c00841>.
2. Novoselov, K.S.; Geim, A.K.; Morozov, S.V.; Jiang, D.; Zhang, Y.; Dubonos, S.V.; Grigorieva, I.V.; Firsov, A.A. Electric field effect in atomically thin carbon films. *Science* **2004**, *306*, 666–669. <https://doi.org/10.1126/science.1102896>.
3. Ferrari, A.C.; Meyer, J.C.; Scardaci, V.; Casiraghi, C.; Lazzeri, M.; Mauri, F.; Piscanec, S.; Jiang, D.; Novoselov, K.S.; Roth, S.; et al. Raman Spectrum of Graphene and Graphene Layers. *Phys. Rev. Lett.* **2006**, *97*, 187401. <https://doi.org/10.1103/PhysRevLett.97.187401>.
4. Amanatiadis, S.; Zygidis, T.; Kantartzis, N. Radiation Efficiency Enhancement of Graphene Plasmonic Devices Using Matching Circuits. *Technologies* **2021**, *9*, 4.

5. Li, J.; Zeng, H.; Zeng, Z.; Zeng, Y.; Xie, T. Promising Graphene-Based Nanomaterials and Their Biomedical Applications and Potential Risks: A Comprehensive Review. *ACS Biomater. Sci. Eng.* **2021**, *7*, 5363–5396. <https://doi.org/10.1021/acsbomaterials.1c00875>.
6. Bouhafs, C.; Stanishchev, V.; Zakharov, A.A.; Hofmann, T.; Kühne, P.; Iakimov, T.; Yakimova, R.; Schubert, M.; Darakchieva, V. Decoupling and ordering of multilayer graphene on C-face 3C-SiC(111). *Appl. Phys. Lett.* **2016**, *109*, 203102. <https://doi.org/10.1063/1.4967525>.
7. Brzhezinskaya, M.; Kononenko, O.; Matveev, V.; Zotov, A.; Khodos, I.I.; Levashov, V.; Volkov, V.; Bozhko, S.I.; Chekmazov, S.V.; Roshchupkin, D. Engineering of Numerous Moiré Superlattices in Twisted Multilayer Graphene for Twistronics and Straintronics Applications. *ACS Nano* **2021**, *15*, 12358–12366. <https://doi.org/10.1021/acsnano.1c04286>.
8. Dien, N.T.; Hirai, Y.; Koshiba, J.; Sakai, S. Factors affecting multiple persistent organic pollutant concentrations in the air above Japan: A panel data analysis. *Chemosphere* **2021**, *277*, 130356. <https://doi.org/10.1016/j.chemosphere.2021.130356>.
9. Zhang, J.; Jia, K.; Huang, Y.; Liu, X.; Xu, Q.; Wang, W.; Zhang, R.; Liu, B.; Zheng, L.; Chen, H.; et al. Intrinsic Wettability in Pristine Graphene. *Adv. Mater.* **2022**, *34*, 2103620. <https://doi.org/10.1002/adma.202103620>.
10. Belyaeva, L.A.; van Deursen, P.M.G.; Barbetsea, K.I.; Schneider, G.F. Hydrophilicity of Graphene in Water through Transparency to Polar and Dispersive Interactions. *Adv. Mater.* **2018**, *30*, 1703274. <https://doi.org/10.1002/adma.201703274>.
11. Ni, Z.H.; Wang, H.M.; Luo, Z.Q.; Wang, Y.Y.; Yu, T.; Wu, Y.H.; Shen, Z.X. The effect of vacuum annealing on graphene. *J. Raman Spectrosc.* **2010**, *41*, 479–483. <https://doi.org/10.1002/jrs.2485>.
12. Yazdi, G.R.; Akhtar, F.; Ivanov, I.G.; Schmidt, S.; Shtepliuk, I.; Zakharov, A.; Iakimov, T.; Yakimova, R. Effect of epitaxial graphene morphology on adsorption of ambient species. *Appl. Surf. Sci.* **2019**, *486*, 239–248. <https://doi.org/10.1016/j.apsusc.2019.04.247>.
13. Kögler, M.; Heilala, B. Time-gated Raman spectroscopy—A review. *Meas. Sci. Technol.* **2020**, *32*, 012002. <https://doi.org/10.1088/1361-6501/abb044>.
14. Craig, R.L.; Bondy, A.L.; Ault, A.P. Surface Enhanced Raman Spectroscopy Enables Observations of Previously Undetectable Secondary Organic Aerosol Components at the Individual Particle Level. *Anal. Chem.* **2015**, *87*, 7510–7514. <https://doi.org/10.1021/acs.analchem.5b01507>.
15. Doughty, D.C.; Hill, S.C. Raman spectra of atmospheric particles measured in Maryland, USA over 22.5 h using an automated aerosol Raman spectrometer. *J. Quant. Spectrosc. Radiat. Transfer* **2020**, *244*, 106839. <https://doi.org/10.1016/j.jqsrt.2020.106839>.
16. Doughty, D.C.; Hill, S.C. Raman spectra of atmospheric aerosol particles: Clusters and time-series for a 22.5 hr sampling period. *J. Quant. Spectrosc. Radiat. Transfer* **2020**, *248*, 106907. <https://doi.org/10.1016/j.jqsrt.2020.106907>.
17. Moorchilot, V.S.; Aravind, U.K.; Menacherry, S.P.M.; Aravindakumar, C.T. Single-Particle Analysis of Atmospheric Aerosols: Applications of Raman Spectroscopy. *Atmosphere* **2022**, *13*, 1779.
18. Liu, Y.; Shi, Y.; Zhou, W.; Shi, W.; Dang, W.; Li, X.; Liang, B. The split-up of G band and 2D band in temperature-dependent Raman spectra of suspended graphene. *Opt. Laser Technol.* **2021**, *139*, 106960. <https://doi.org/10.1016/j.optlastec.2021.106960>.
19. Yang, M.; Wang, L.; Qiao, X.; Liu, Y.; Shi, Y.; Wu, H.; Liang, B.; Li, X.; Zhao, X. Temperature Dependence of G and D' Phonons in Monolayer to Few-Layer Graphene with Vacancies. *Nanoscale Res. Lett.* **2020**, *15*, 189. <https://doi.org/10.1186/s11671-020-03414-w>.
20. Linas, S.; Magnin, Y.; Poinso, B.; Boisson, O.; Förster, G.D.; Martinez, V.; Fulcrand, R.; Tournus, F.; Dupuis, V.; Rabilloud, F.; et al. Interplay between Raman shift and thermal expansion in graphene: Temperature-dependent measurements and analysis of substrate corrections. *Phys. Rev. B* **2015**, *91*, 075426. <https://doi.org/10.1103/PhysRevB.91.075426>.
21. Cunha, R.; Perea-López, N.; Elías, A.L.; Fujisawa, K.; Carozo, V.; Feng, S.; Lv, R.; dos Santos, M.C.; Terrones, M.; Araujo, P.T. Probing the interaction of noble gases with pristine and nitrogen-doped graphene through Raman spectroscopy. *Phys. Rev. B* **2018**, *97*, 195419. <https://doi.org/10.1103/PhysRevB.97.195419>.
22. Valeš, V.; Kovaříček, P.; Fridrichová, M.; Ji, X.; Ling, X.; Kong, J.; Dresselhaus, M.; Kalbác, M. Enhanced Raman scattering on functionalized graphene substrates. *2D Mater.* **2017**, *4*, 025087. <https://doi.org/10.1088/2053-1583/aa6b6e>.
23. Hung, Y.-J.; Hofmann, M.; Cheng, Y.-C.; Huang, C.-W.; Chang, K.-W.; Lee, J.-Y. Characterization of graphene edge functionalization by grating enhanced Raman spectroscopy. *RSC Adv.* **2016**, *6*, 12398–12401. <https://doi.org/10.1039/C5RA21717B>.
24. Yang, G.; Li, L.; Lee, W.B.; Ng, M.C. Structure of graphene and its disorders: A review. *Sci. Technol. Adv. Mater.* **2018**, *19*, 613–648. <https://doi.org/10.1080/14686996.2018.1494493>.
25. Mazumder, M.; Das, R.; Sajib, M.S.J.; Gomes, A.J.; Islam, M.; Selvaratnam, T.; Rahman, A. Comparison of Different Hydrotalcite Solid Adsorbents on Adsorptive Desulfurization of Liquid Fuel Oil. *Technologies* **2020**, *8*, 22.

Disclaimer/Publisher's Note: The statements, opinions and data contained in all publications are solely those of the individual author(s) and contributor(s) and not of MDPI and/or the editor(s). MDPI and/or the editor(s) disclaim responsibility for any injury to people or property resulting from any ideas, methods, instructions or products referred to in the content.